Rupture and healing of one-dimensional chains in a parametric magnetic ratchet potential

Pietro Tierno,[1] Sathavaram V. Reddy,[1] Tom H. Johansen,[2] and Thomas M. Fischer[1,*]
[1]*Department of Chemistry and Biochemistry, Florida State University, Tallahassee, Florida 32306, USA*
[2]*Department of Physics, University of Oslo, P. O. Box 1048, Blindern, Norway*
(Received 13 December 2006; published 17 April 2007)

Transverse paramagnetic particle chains parametrically driven by a magnetic ratchet potential rupture and heal upon collision with an obstacle. The overdamped transverse dynamics is frozen during the time the particles stay in the ratchet potential wells and kicked during the time the particles hop to the next well. On time scales large compared to the parametric modulation period the healing of the hole in the chain is determined by dipolar repulsion and hydrodynamic friction of the paramagnetic particles.

DOI: 10.1103/PhysRevE.75.041404 PACS number(s): 82.70.Dd, 07.07.Df

I. INTRODUCTION

Colloidal particles can be assembled into a rich variety of organized structures [1–4]. They also provide an interesting model for the study of different kinds of dissipative dynamics, because typical length and time scales lie in an experimentally accessible range [5,6]. The net transport of particles using a ratchet mechanism has received considerable interest because it is also the working principle of molecular motors such as myosin or actin [7–9]. There are different experimental methods to confine colloidal particles into a potential well. Wei, Bechinger, and Leiderer [10] and Cui, Diamant, and Lin [11] have used hard walls fabricated by photolithographic techniques to confine colloidal particles into circular trenches or narrow channels. Lee and Grier [12] used holographic optical tweezers to realize one-dimensional (1D) thermal ratchets. Helseth *et al.* [6] showed that localized magnetic potential wells can be also used to effectively trap paramagnetic colloidal particles. When an aqueous solution of the particles is placed on top of a ferrimagnetic garnet film, the particles are pinned to the domain walls of the film by the stray magnetic field. These magnetic potential wells can be used to create parametrically driven ratchets since they can be easily manipulated by using external magnetic fields. In this context, we recently developed a parametric ratchet that allows the dispersion-free programmable motion of a large assembly of paramagnetic particles [13]. In the present work we study the transverse kinetics of a colloidal particle chain moved across the ratchet potential, enforcing a collision with an impenetrable obstacle made by a drop of oil. The domains of a magnetic garnet film with uniaxial anisotropy provide a magnetic field above the film serving as a ratchet potential. When the particle chain collides with the oil drop, the chain divides into two compressed 1D chains that are separated by a finite distance. After passing the droplet, the hole closes and the two chains reexpand in steps during the periods while the chain is hopping from one well to the next. A finite amount of steps is needed for the two chains to recombine into the original line.

II. EXPERIMENTAL METHODS

The magnetic ratchet potential was created by the stripe domain pattern of a ferrimagnetic garnet film which was grown epitaxially on a gadolinium gallium garnet (GGG) substrate [14,15]. The garnet film had a composition $Y_{2.5}Bi_{0.5}Fe_{5-q}Ga_qO_{12}$ ($q=0.5-1$), a thickness of ~ 5 μm and a saturation magnetization $M_s=1.7\times10^4$ A/m. Upward and downward magnetized domains periodically repeat with a wavelength $\lambda=10.9$ μm, which is 2 times the domain width. Application of a magnetic field perpendicular to the film increases the width of the domains with magnetization parallel to the field and decrease the width of antiparallel domains. Paramagnetic polystyrene particles with a mean radius $a=0.5\pm0.3$ μm, a density of $\rho=1.4$ g/cm^3 and an effective magnetic susceptibility $\chi=0.3$ (Dynabeads, Myone) were dispersed in H_2O at a concentration of $\sim 2\times10^9$ beads/ml. The particles were electrostatically stabilized by the negative charges acquired from the dissociation of the surface carboxylic groups (COO-). We diluted the original particle solution with deionized water (18.2 MΩ cm, MilliQ system) to a concentration of $\sim 10^7$ particles/ml. This solution was then mixed one to one with a 1.02% water dispersion of silicon oil (Fisher Scientific). The silicon oil has a density of 0.96 g/ml and an interfacial tension with water of $\gamma_{ow}=36.5$ mN/m [16]. Sonication for 30 minutes formed an emulsion of oil droplets in water which was then placed on top of the garnet film. To prevent the particles from adhering to the surface of the garnet film, the film was coated with a thin layer of polysodium 4-styrene sulfonate by using the layer-by-layer adsorption technique [6]. After 5 minutes the particles sediment above the garnet surface and are attracted by the magnetic domain walls. The oil droplets, with diameter ranging from 1 to ~ 20 μm, partially wet the film surface by forming spherical caps. The external magnetic field was applied by using two coils with the main axes along the x and z direction, and field modulations were achieved by using a wave generator feeding an amplifier connected to the coils. The particles and the droplets were observed using an optical microscope (Leica, DMLP). The magnetic domain pattern of the garnet film was visualized with polarization microscopy making use of the polar Faraday effect. Videos of the colloidal chain kinetics were taken at 125 fps with a black and white camera (Fastcam Super 10 K Photron) or at 30 fps with a color camera (Basler, VT).

*Electronic address: tfischer@chem.fsu.edu

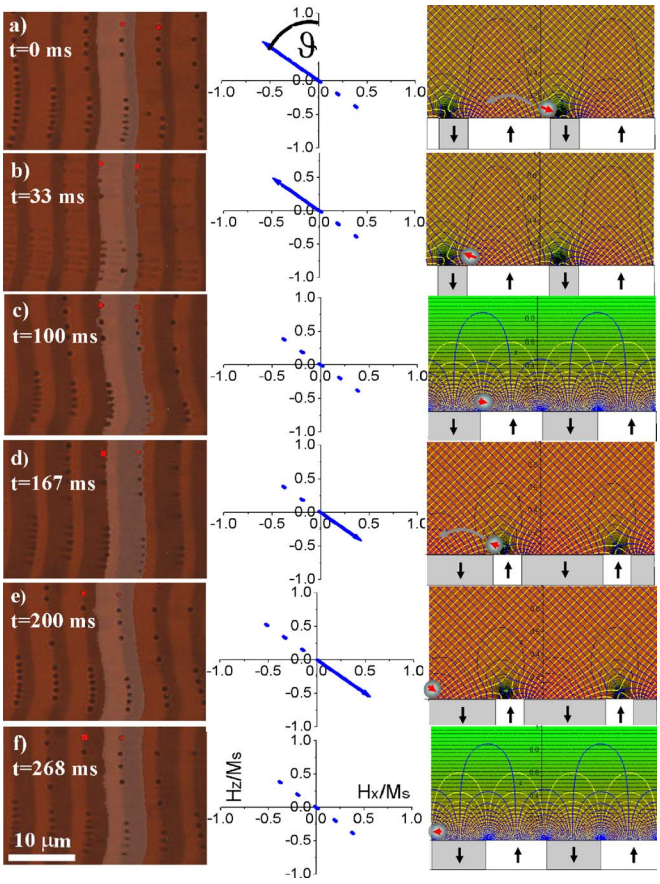

FIG. 1. (Color online) (Left-hand side) Sequence of polarization microscope images showing the motion of paramagnetic particles on top of a garnet film. Two particles are marked in (red) gray and two stripes are shaded in white. (Middle) Direction and amplitude of the external magnetic field. (Right-hand side) Magnetic field lines [(blue) gray], equipotential lines [(yellow) white], and magnetic energy of the particles [shaded from (red to green) white to gray] above the magnetic garnet film. A video clip of the hopping across the stripes can be found in [17].

III. PARTICLE MOTION IN THE PARAMETRIC RATCHET

In Ref. [13] we used the parametric ratchet potential for the digital transport of biomolecular cargo bound to the paramagnetic particles. Here we describe the details of the parametric ratchet. Figure 1 displays consecutive polarization microscope images of paramagnetic particles moving above a garnet film of wavelength λ. The linearly polarized external magnetic field oscillates harmonically in the (x,z) plane with an angular frequency ω, inclination ϑ with respect to the film normal, and amplitude $\hat{\mathbf{H}}_{\text{ext}}=H_0(\sin\vartheta,0,\cos\vartheta)$ (here $H_0=1.3\times10^4$ A/m, $\vartheta=-45°$). The direction and magnitude of the field are shown in the second column of Fig. 1. Upward magnetized domains appear brighter than downward magnetized domains. One period of upward and downward stripes is artificially shaded as a guide through the sequence of images. Paramagnetic particles appear as dark circles slightly shifted toward the majority domain at the domain wall boundaries. To guide the eye two particles are marked in (red) gray. As a result of the magnetic field modulation the domain walls and the paramagnetic particles respond with a motion parallel to the film plane. The motion consists of periods, where the particles are pinned to the moving domain walls and periods where the particles detach from one domain wall, cross one domain, and hop to the next domain wall. The motion of the domain walls is periodic such that each domain wall returns to its initial position after one cycle $T=2\pi/\omega$. The particles' position, on the other hand, is not periodic and advances by one wavelength of the stripe pattern after one cycle. The particles pin to the domain walls when the external field is small $(\omega t\approx\pi/2+n\pi, n=0,1,2,3,\ldots)$ and hop to the next domain wall during the times of maximum intensity of the external field $(\omega t\approx n\pi, n=0,1,2,3,\ldots)$. The hopping across the domains occurs randomly in a forward or backward direction if the external field is normal to the surface $\vartheta=0$. However with a finite external field inclination $\vartheta<0$ $(\vartheta>0)$, the particles strictly hop in the negative (positive) x direction. A video clip underlining the ratchet motion of the particles is available in [17].

The motion of the particles can be explained by the magnetic energy landscape created by the external magnetic field and the inhomogeneous field of the garnet film. For stripes strictly aligned along the y direction, the magnetic field above the garnet film is a solution of the two-dimensional Laplace equation, and so we may use the technique of conformal mapping. For convenience we work with dimensionless quantities and scale the magnetic field by the magnetization of the garnet film, and the distance by the wavelength λ. Since the curl of the magnetic field vanishes above the garnet film we may express the total magnetic field as the gradient of a magnetic potential $\mathbf{H}=\nabla\,\mathrm{Re}(\psi)$, where the potential function ψ reads:

$$\psi=\frac{i}{\pi^2}[\mathrm{dilog}(1-e^{\{(i\pi/2)[4w+\mathrm{Im}(h)]\}}) - \mathrm{dilog}(1+e^{\{(i\pi/2)[4w-\mathrm{Im}(h)]\}})]+w\cdot h \qquad (1)$$

with $w=x+iz$, $h=\mathbf{H}_{\text{ext}}\cdot(\hat{e}_x-i\hat{e}_z)$ and the dilogarithmic function $\mathrm{dilog}(z)=\int_1^z\frac{d\zeta\ln\zeta}{1-\zeta}$. The potential ψ ensures that the magnetic field reduces to the external field for $z\to\infty$ and that the normal component of the magnetic field just above the garnet film coincides with the magnetization of the stripes below, i.e., $+M_s(-M_s)$ for a domain with upward (downward) magnetization direction. The magnetic field lines are given by $\mathrm{Im}(\psi)=\text{const}$ and they are cut orthogonal by the lines of constant magnetic potential, $\mathrm{Re}(\psi)=\text{const}$.

On the right-hand side of Fig. 1 we plot the magnetic field lines (blue or gray), the magnetic potential lines (yellow or white), and the magnetic energy $E\propto H^2$ (shaded from red to green or from white to green) for different times t. The particles are located where the magnetostatic energy is minimum, that is above the *strong* domain walls where the x component of the external field points in the same direction as the field from the garnet film, thus increasing the total field strength. As we modulate the external field the domain walls periodically switch between being strong and weak

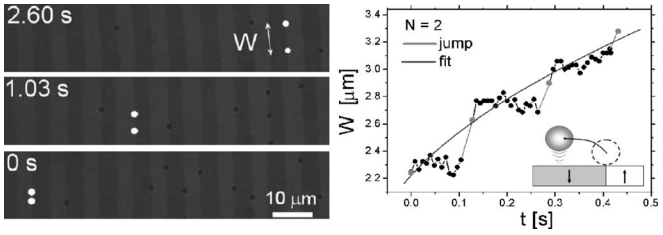

FIG. 2. Left-hand side: Sequence of images showing the longitudinal ratchet motion and the transverse separation of two paramagnetic particles (in white). Right-hand side: Transverse separation W of the two particles as a function of time. The inset shows a schematic of the particle hopping from one domain wall to the next. The (blue) gray line is a theoretical fit of the (red) gray points according to the dynamics predicted by Eq. (3).

domain walls. A particle pinned to an originally strong wall will hop to the next wall as the original wall becomes weak. In principle the particle could jump backward or forward to the next strong wall. However the presence of the normal component of the external field also turns either the upward or downward magnetized domains into a majority domain. The field strength above the majority domain is stronger than above the minority domain and the particle hop across the majority domain, which is always to the left-hand side (right-hand side) of the weak domain wall if the inclination angle of the external field is smaller (larger) than zero.

IV. TRANSVERSE CHAIN KINETICS

A. Dipolar dispersion

In Fig. 2 we show the kinetics of two paramagnetic particles travelling in the same magnetic potential well. The parametric ratchet induces a particle motion perpendicular to the stripe pattern. Since the ratchet motion strictly enforces the particles to move exactly one wavelength during one field cycle, the longitudinal motion is free of dispersion, thus ensuring that both particles do not separate along the direction of motion. Due to the magnetic field above the film a magnetic moment is induced in each of the particles and the particles experience repulsive dipolar interactions. These interactions cause transverse dispersion of the particles and they separate (in stripe direction) with time. The separation kinetics is a kicked kinetics. Significant transverse separation of the particles only occurs during the short periods, when the particles hop from one well to the next. The transverse kinetics is frozen when the particles are trapped in one of the wells.

A sphere of radius a traveling in a liquid of viscosity η with velocity v parallel to a wall experiences a frictional force, $F_h = \eta f a v$ with a friction coefficient $f = -6\pi \ln(z/a - 1)$ which strongly increases as the sphere move closer to the wall surface. Here z is the elevation of the particle center above the garnet surface [18]. To explain the kicked transverse kinetics we observe that when the particles are trapped in the magnetic potential well they are very close to the garnet surface, while they elevate during hopping (see schematic in Fig. 2).

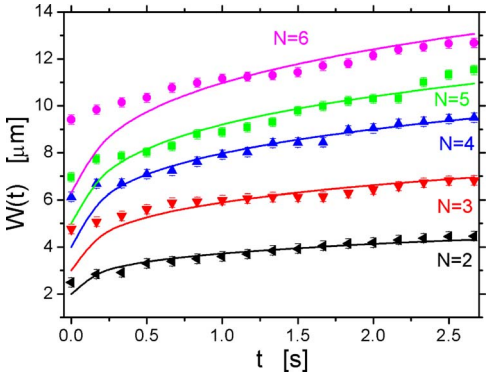

FIG. 3. (Color online) Chain width W as a function of time for different chains consisting of $N = 1, \ldots, 6$ particles. Each point is taken right after hopping of the chain to the next domain wall. The solid lines are theoretical fits according to Eq. (3).

The kinetics on time scales exceeding the parametric modulation period is smooth. In Fig. 3 we plot the long time kinetics of the transverse width W for chains consisting of different number of particles ($N = 1, \ldots, 6$). We used a stroboscopic recording: each point in Fig. 3 was taken right after the hopping of the particle chain to the next domain wall.

In what follows we give an explanation of the long time kinetics by a balance of dipolar and hydrodynamic forces. Upon application of an external magnetic field $\mathbf{H}$ each particle can be considered as a point dipole. The induced moment is related to the magnetic field by $\mathbf{m} = (4\pi/3)a^3\chi\mathbf{H}$, where χ is the effective magnetic susceptibility and a the radius of the particle. This relation holds for the magnetic field strengths applied here that are well below the saturation magnetization of the particles [19]. If we consider a chain made by N particles at positions y_i and separated in a direction normal to the magnetic field by distances $\mathbf{d}_{ij}$, the total magnetic energy of the chain can be written as

$$U_m = \frac{\mu_0}{4\pi} \sum_{j>i}^{N} \sum_{i=1}^{N-1} U_{ij}, \quad U_{ij} = \frac{\mathbf{m}_i \cdot \mathbf{m}_j}{d_{ij}^3}, \tag{2}$$

where the separation distances $d_{ij} = |y_i - y_j|$ depend on the relative position of the magnetic moments $\mathbf{m}_i$ and $\mathbf{m}_j$. The dipoles are aligned along the direction of the total magnetic field $\mathbf{H}$ which in our experiments is given by the external field plus the stray magnetic field of the garnet film. Assuming a uniform separation of the particles the expansion of the 1D chain results from a balance of the dipolar force $F_m = -\partial U_m / \partial d$ and the hydrodynamic force F_h. Following the analysis of Helseth *et al.* [20] we find that

$$W(t) = 2a[1 + (N-1)(1 + At)^{1/5}], \tag{3}$$

where $A = \frac{5\pi\mu_0\chi^2 H^2}{12\eta f} \Sigma_{i=1}^{N-1} \frac{1}{i^4}$. Here μ_0 is the vacuum permeability. In Figs. 2 and 3, fits of the experimental data according to Eq. (3) are added as continuous lines. The fits agree well with the experiment supporting the theoretical analysis. Note, that the transverse kinetics, as observed in Fig. 2, happens on a time scale larger than the one shown in Fig. 1 and therefore it is not detectable in Fig. 1.

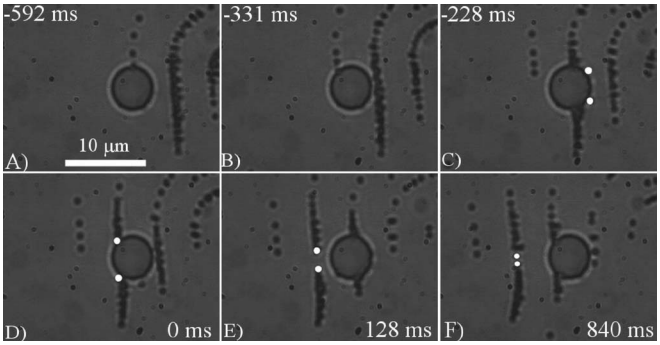

FIG. 4. Series of microscope images showing a 1D monolayer of paramagnetic particles colliding with an oil drop. As a guide for the eye the two outermost particles are marked in white. The particles move from right to left.

B. Hole closure

We can use the ratchet mechanism illustrated in Sec. IV A to direct chains of paramagnetic particles onto obstacles located on top of the garnet film. As an obstacle we use a droplet of oil that partially wets the garnet film forming a spherical cap. Figure 4 shows a series of microscope images of a colloidal chain consisting of $N=28$ paramagnetic particles parametrically driven across the garnet film and colliding against an oil cap of diameter $D=5.3$ μm. Each time step corresponds to one-half cycle of the parametric modulation and the progression of the particles by one domain wall. At times $t=-592$ ms and $t=-331$ ms the particle chain is advancing toward the oil droplet, then it impacts on the droplet and at $t=-228$ ms the chain divides into two separate and compressed lines consisting of $N_1=16$ and $N_2=12$ particles. We have marked the two particles moving along the water-oil interface in white to guide the eye. During collision these two particles slide along the oil surface and, when the chain leaves the droplet at $t=0$, a *hole* has formed. The size of the hole is dictated by the drop diameter D. After the particles have passed the droplet, the two compressed chains start to reexpand. A movie showing the collision of the chain with the droplet and the healing of the chain after the collision can be found in [17]. We measured the width h of the hole and the result is shown in Fig. 5. To obtain an expression for the time dependence of h we use the theory outlined in Sec. IV A. We neglect the dipolar interaction between the separated chains and apply Eq. (3) to each separated chain individually. For $t>0$ the widths $W_i(t)$ $(i=1,2)$ of the two chains starts to expand symmetrically according to Eq. (3), until the hole width returns to the equilibrium interparticle distance $h=d$ of an N_1+N_2 particle chain. We therefore predict a hole closure dynamics given by

$$h(t) = D + a(N_1 + N_2) - \tfrac{1}{2}[W_1(t) + W_2(t)]. \qquad (4)$$

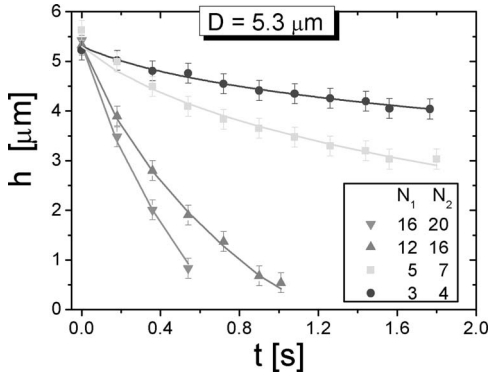

FIG. 5. Hole width h as a function of time t for pairs of separated chains of varying particle number N_1 and N_2. The diameter of the oil drop is $D=5.3$ μm. The solid lines are fits according to Eq. (4) using friction coefficients in the range of $f=80\pm5$.

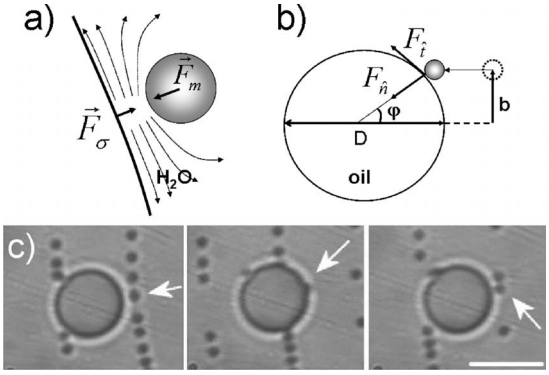

FIG. 6. Schematic illustrations showing a particle incident against an oil drop. (a) Illustration of the lubrication forces preventing capillary trapping of the particles. The direction of the tangential force in (b) decides whether the droplet slides along the droplet surface as in Fig. 4 or whether it rebounds like the particle marked in the following image sequence. (c) Sequence of images showing the rebound of a particle colliding with the droplet with a low collision parameter b. The images are separated in time by 0.17 s each and the scale bar is 10 μm.

We use Eq. (4) to fit the experimental data of Fig. 5 (continuous line) and we find good agreement using friction coefficients in the range of $f=80\pm5$ corresponding to an elevation of the particles by $z=a+7$ nm. As expected, $h(t)$ depends on the size of the chains; larger chains relax faster than shorter chains reflecting the roughly linear increase of dipolar interaction with the lengths of the two chains. Long chains like those shown in Fig. 4 recombine after very few steps. For very short chains, like for $N_1=3$ and $N_2=4$, the recombination of both chains cannot be observed since the two chains move out of the field of view before they recombine.

V. COLLISION DYNAMICS

The magnetic forces acting on the paramagnetic particles in the parametric ratchet are in the *pN* range. Since the particles detach from the oil droplet as shown in Fig. 4, or bounce back from the oil droplet as the marked particle in Fig. 6(c), it is clear that the particles do not penetrate into the water-oil interface. Capillary forces are of the order of 100 nN and, once a particle was captured by the interface, the magnetic ratchet forces would be too weak to free the particles from the interface. As shown in Fig. 6(a), hydrody-

namic lubrication forces prevent the particles from getting trapped at the water-oil interface. Such lubrication forces are proportional to the speed of approach to the interface and diverge with the size of the gap between the interface and the particle. It is therefore essential that the ratchet drives the particles fast enough along the water-oil interface so that they have no time to relax into the more stable interfacial position. Yet it is known that oil-water interface can acquire negative charges in absence of surfactant [21]. Electrostatic repulsion between accumulated charges on the droplet and ions present in the particles' double layer further prevent interfacial particle entrapment.

VI. CONCLUSIONS

In this work we have reported on the rupture and healing of traveling dipolar chains colliding with a spherical drop of oil located on top of the surface. The chains were made by paramagnetic particles hopping between domain walls of a ferrimagnetic garnet film. The transverse relaxation of the chains is kicked and occurs only during the hopping periods. During these periods the relaxation is determined by a balance of hydrodynamic and dipolar interactions. The ratchet motion is fast enough to prevent capillary trapping of the particles at the water-oil interface of the droplet. Our magnetic ratchet may be of interest for microfluidic applications.

ACKNOWLEDGMENT

The authors acknowledge Colin Byfleet for a critical reading of the paper. T.H.J. thanks the Research Council of Norway for financial support.

[1] A. van Blaaderen, R. Ruel, and P. Wiltzius, Nature (London) **385**, 321 (1997).
[2] M. Adams, Z. Dogic, S. L. Keller, and S. Fraden, Nature (London) **393**, 349 (1998).
[3] R. C. Hayward, D. A. Saville, and I. A. Aksay, Nature (London) **404**, 56 (2000).
[4] P. Schall, I. Cohen, D. A. Weitz, and F. Spaepen, Nature (London) **440**, 319 (2006).
[5] V. J. Anderson and H. Lekkerkerker, Nature (London) **416**, 811 (2002).
[6] L. E. Helseth, H. Z. Wen, T. M. Fischer, and T. H. Johansen, Phys. Rev. E **68**, 011402 (2003).
[7] I. Y. Wong, M. L. Gardel, D. R. Reichman, E. R. Weeks, M. T. Valentine, A. R. Bausch, and D. A. Weitz, Phys. Rev. Lett. **92**, 178101 (2004).
[8] L. Le Goff, F. Amblard, and E. M. Furst, Phys. Rev. Lett. **88**, 018101 (2001).
[9] P. Lenz, J.-F. Joanny, F. Julicher, and J. Prost, Phys. Rev. Lett. **91**, 108104 (2003).
[10] Q.-H. Wei, C. Bechinger, and P. Leiderer, Science **287**, 625 (2000).
[11] B. Cui, H. Diamant, and B. Lin, Phys. Rev. Lett. **89**, 188302 (2002).
[12] S. Lee and D. G. Grier, J. Phys.: Condens. Matter **17**, S3685 (2006).
[13] P. Tierno, S. V. Reddy, M. Roper, T. H. Johansen, and T. M. Fischer (unpublished).
[14] L. E. Helseth, T. Backus, T. H. Johansen, and T. M. Fischer, Langmuir **21**, 7518 (2005).
[15] K. L. Babcock and R. M. Westervelt, Phys. Rev. A **40**, 2022 (1989).
[16] P. Erni, P. Fischer, and E. J. Windhab, Ann. Trans. Nordic Rheology Society **12**, 175 (2004).
[17] See EPAPS Document No. E-PLEEE8-75-187703 for video clips of experimental observations. For more information on EPAPS, see http://www.aip.org/pubservs/epaps.html.
[18] W. B. Russel, D. A. Saville, and W. R. Schowalter, *Colloidal Dispersions* (Cambridge University Press, Cambridge, 1995), p. 51.
[19] P. Tierno and W. A. Goedel, J. Chem. Phys. **122**, 094712 (2005).
[20] H. W. L. E. Helseth and T. Fischer, J. Appl. Phys. **99**, 024909 (2006).
[21] J. C. Carruthers, Trans. Faraday Soc. **34**, 300 (1938).